Anal Bioanal Chem (2013) 405:1705–1712
DOI 10.1007/s00216-012-6584-4

ORIGINAL PAPER

Investigation of the metabolism of monepantel in ovine hepatocytes by UHPLC/MS/MS

Lucie Stuchlíková · Robert Jirásko · Ivan Vokřál · Jiří Lamka · Marcel Špulák · Michal Holčapek · Barbora Szotáková · Hana Bártíková · Milan Pour · Lenka Skálová

Received: 11 October 2012 / Revised: 14 November 2012 / Accepted: 14 November 2012 / Published online: 25 November 2012

Abstract Monepantel (MOP) belongs to a new class of anthelmintic drugs known as aminoacetonitrile derivatives. It was approved for use in veterinary practice in Czech Republic in 2011. So far, biotransformation and transport of MOP in target animals have been studied insufficiently, although the study of metabolic pathways of anthelmintics is very important for the efficacy of safety of therapy and evaluation of the risk of drug–drug interactions. The aim of this study was to identify MOP metabolites and to suggest the metabolic pathways of MOP in sheep. For this purpose, primary culture of ovine hepatocytes was used as a model in vitro system. After incubation, medium samples and homogenates of hepatocytes were extracted separately using solid-phase extraction. Analysis was performed using a hybrid quadrupole-time-of-flight analyzer with respect to high mass accuracy measurements in full scan and tandem mass spectra for the confirmation of an elemental composition. The obtained results revealed S-oxidation to sulfoxide and sulfone and arene hydroxylation as MOP phase I biotransformations. From phase II metabolites, MOP glucuronides, sulfates, and acetylcysteine conjugates were found. Based on the obtained results, a scheme of the metabolic pathway of MOP in sheep has been proposed.

Keywords Monepantel · Aminoacetonitrile derivatives · Ultrahigh-performance liquid chromatography/mass spectrometry · Biotransformation · Drug metabolism

Abbreviations

AADs	Aminoacetonitrile derivatives
BSA	Bovine serum albumin
DMSO	Dimethyl sulfoxide
EGTA	Ethylene glycol-bis (β-aminoethyl ether) *N*,*N*,*N*′,*N*′-tetraacetic acid
ESI	Electrospray ionization
HPLC	High-performance liquid chromatography
MOP	Monepantel
MOP.OH	Monepantel with hydroxylation
MOP.SO	Monepantel sulfoxide
MOP.SO.OH	Monepantel sulfoxide with hydroxylation
$MOP.SO_2$	Monepantel sulfone
$MOP.SO_2.OC_6H_9O_6$	Glucuronide of hydroxylated monepantel sulfone
$MOP.SO_2.OH$	Monepantel sulfone with hydroxylation

L. Stuchlíková · B. Szotáková · H. Bártíková · L. Skálová (✉)
Department of Biochemical Sciences, Faculty of Pharmacy in Hradec Králové, Charles University in Prague, Heyrovského 1203, 500 05 Hradec Králové, Czech Republic
e-mail: skaloval@faf.cuni.cz

R. Jirásko · M. Holčapek
Department of Analytical Chemistry, Faculty of Chemical Technology, University of Pardubice, Studentská 573, 532 10 Pardubice, Czech Republic

I. Vokřál · J. Lamka
Department of Pharmacology and Toxicology, Faculty of Pharmacy in Hradec Králové, Charles University in Prague, Heyrovského 1203, 500 05 Hradec Králové, Czech Republic

M. Špulák · M. Pour
Department of Inorganic and Organic Chemistry, Faculty of Pharmacy in Hradec Králové, Charles University in Prague, Heyrovského 1203, 500 05 Hradec Králové, Czech Republic

$MOP.SO_2.OH.OC_6H_9O_6$	Glucuronide of dihydroxylated monepantel sulfone
$MOP.SO_2.OSO_3H$	Sulfate of hydroxylated monepantel sulfone
$MOP.SO_2.SC_5H_8NO_3$	Monepantel sulfone conjugated with acetylcysteine
MS	Mass spectrometry
MS/MS	Tandem mass spectrometry
NMR	Nuclear magnetic resonance
PPTS	Pyridinium *p*-toluenesulfonate
QqTOF	Quadrupole-time-of-flight analyzer
RP	Reversed-phase
SPE	Solid-phase extraction
t-BuOK	Potassium *tert*-butoxide
THF	Tetrahydrofuran
THP	Tetrahydropyran-2-yl
UHPLC	Ultrahigh-performance liquid chromatography

Introduction

A major problem facing the agriculture industry and human health is the battle against parasitic helminths. Anthelmintics remain the sole accessible means in helminthoses therapy, but only a limited number of chemical groups of broad-spectrum anthelmintics is available. The treatment of helminthoses is mainly based on the administration of anthelmintic drugs from the following groups: benzimidazoles (e.g., flubendazol, albendazol, and fenbendazol), imidazothiazoles (e.g., levamisole), and macrocyclic lactones (e.g., ivermectin) [1]. The frequent use of similar anthelmintics over many years has inevitably led to the development of drug resistance in some helminths [2, 3]. This phenomenon is a serious problem worldwide and causes extensive economic losses. Therefore, the development of new class of anthelmintics is extremely important [2, 4].

In 2008, the preparation and promising anthelmintic efficacy of amino-acetonitrile derivatives (AADs) has been reported. AADs, low-molecular-mass compounds, were prepared by the alkylation of phenol with chloroacetone followed by Strecker reaction on the resulting ketone and a final acylation step of the amino group using an acid chloride [5, 6]. These compounds have aryloxy and aroyl moieties on an amino-acetonitrile core [7]. AADs have met requirements for the treatment of helminthoses in livestock: low toxicity, favorable pharmacokinetic properties, and broad-spectrum efficacy against sheep and cattle nematodes [5]. At this time, one AADs representative—monepantel—has been approved for use in veterinary practice (Fig. 1). For the determination of AADs including monepantel in biological samples, high-performance liquid chromatography with tandem mass spectrometry (HPLC/MS/MS) method with the negative-ion electrospray ionization (ESI) was employed [7, 8].

Safe and effective therapy and limitation of drug–drug interactions require not only information about pharmacokinetic of parent drug but also detailed knowledge of drug metabolism in target species. HPLC/MS/MS is usually a method of choice for the metabolic studies due to high sensitivity and structural information even for trace metabolites in highly complex matrices [9]. The ongoing development on HPLC/MS/MS including ultrahigh-performance liquid chromatography (UHPLC) has opened up new strategies for the veterinary drug residue analysis [7, 10–12]. Several strategies, such as the use of selected tandem mass spectrometry (MS/MS) scans [9, 13–15], online hydrogen/deuterium exchange HPLC/MS/MS [13], accurate mass measurements [9, 15], radio-labeling of parent-drugs [16], chemical derivatization to determine the metabolite position or to improve ionization efficiency [13, 14], and software dedicated to the metabolite prediction or detection [15] can be applied for this purpose.

Monepantel sulfone is the only metabolite of monepantel reported so far. In sheep, monepantel sulfone was found in milk and muscle [7]. Detection of monepantel sulfoxide, presumable intermediate of monepantel sulfone, in the preliminary study was mentioned (unpublished data of Jung et al., see in [8]). No information about phase II metabolites of MOP has been available yet. Therefore, the goal of present study is the identification of all phase I and phase II metabolites in sheep using the primary culture of ovine hepatocytes. For this purpose, the extraction procedure for MOP and its metabolites was developed and UHPLC/MS/MS method for the identification of MOP metabolites was optimized.

Materials and methods

Animals

Sheep (*Ovis* sp.) were bred in the farm Běleč (Czech Republic). For experiments, male castrated lambs (body weight approximately 20 kg; age 9 months) were used. All experimental procedures were undertaken in accordance with the Czech guidelines for the care and use of farm and experimental animals and were performed under the supervision of Ethical Committee of the Charles University in Prague, Faculty of Pharmacy in Hradec Králové.

Chemicals and reagents

Monepantel was prepared at the Department of Organic Chemistry (Faculty of Pharmacy in Hradec Králové, Charles University in Prague, Czech Republic) according to

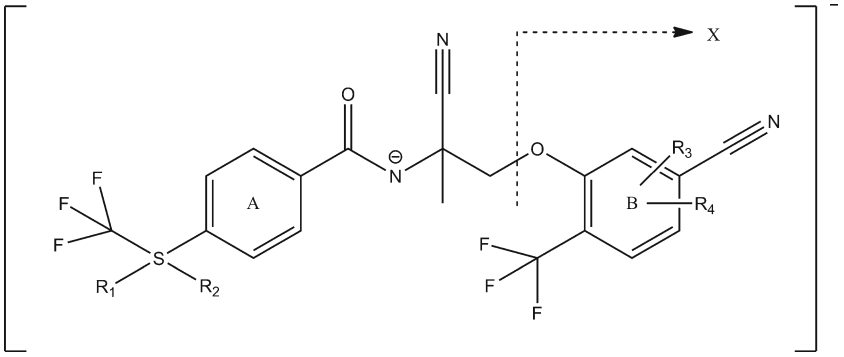

Fig. 1 Chemical structure of monepantel (MOP), *N*-[(1S)-1-cyano-2-(5-cyano-2-trifluoromethyl-phenoxy)-1-methyl-ethyl]-4-trifluoromethylsulfanyl-benzamide, product ions, and substituents of metabolites of phase I and II biotransformation (see Table 2)

Kaminsky et al. [5] with minor modifications. The starting hydroxyacetone was firstly converted to tetrahydropyran-2-yl (THP) ether in 79 % yield followed by Strecker reaction employing potassium cyanide, ammonium chloride, and ammonia solution in ethanol affording the product in 70 % yield. The resultant amino-acetonitrile was converted to its (4-trifluoromethylsulfanyl) benzamide derivative by the reaction of appropriate benzoyl chloride (71 % yield), and then THP protecting group was cleaved in slightly acidic conditions (pyridinium *p*-toluenesulfonate (PPTS)/methanol, 97 % yield). The last step involved nucleophilic aromatic substitution with 4-fluoro-3-trifluoromethylbenzonitrile and alcoholate, in situ released by the fresh solution of *t*-BuOK in THF from AAD (27 %). The structure and purity of prepared substance was tested using NMR and liquid chromatography with mass spectrometry. Liquid sterile-filtered medium Ham F12, Williams' medium, bovine serum albumin (BSA), ethylene glycol-bis(β-amino-ethyl ether) *N, N, N′, N′*-tetra acetic acid (EGTA), and other chemicals (UHPLC, MS, or analytical grade) were obtained from Sigma-Aldrich (St. Louis, MO, USA). Collagenase was purchased from Sevapharma (Prague, Czech Republic).

Preparation of primary culture of ovine hepatocytes

Lamb was stunned and exsanguinated in agreement with Czech slaughtering rules for farm animals. After removal of the liver from the abdominal cavity (up to 5 min), the liver was flushed with Euro Collins solution (15 mM KH_2PO_4, 42.5 mM K_2HPO_4, 15 mM KCl, 10 mM $NaHCO_3$, and 0.2 M glucose) through the main veins and transported to the laboratory on ice (within 60 min). The ovine hepatocytes were obtained from the ovine liver by two-step collagenase method [17, 18]. Briefly, left lobe (100–150 g) was perfused with salt solution (0.14 M NaCl, 5.0 mM KCl, 0.8 mM $MgSO_4$) in Na^+/K^+ phosphate buffer (0.2 mM, pH 7.4) containing a calcium binding component (0.4 mM EGTA). Consequently, the lobe was perfused with phosphate buffer containing calcium chloride (1.46 mM) and collagenase (30 mg/100 mL) at 37 °C. The collagenase perfusion was proceeded 8–10 min. After perfusion, the lobe was transferred to medium containing BSA, and the hepatocytes were released. The obtained suspension was filtered through a nylon mesh and centrifuged at 40×*g* for 5 min at 4 °C. The pellet was re-suspended in chilled buffer, and the washing procedure was twice repeated. Finally, three millions of viable (75–80 %) cells in 3 mL of culture medium ISOM (1:1 mixture of Ham F12 and Williams' E) were placed into 60 mm plastic dishes pre-coated with collagen. The fetal calf serum was added in the culture medium (5 %). Cultures were maintained without the substrate for 4 h at 37 °C in a humid atmosphere of air and 5 % CO_2.

Incubation of hepatocytes with monepantel and solid-phase extraction

After the attachment of hepatocytes, the medium was replaced with a fresh serum-free one with monepantel (10 μM in 3 mL of fresh medium). Monepantel was predissolved in dimethyl sulfoxide (DMSO). The final concentration of DMSO in the medium did not exceed 0.2 %. After 24 h, the hepatocytes were scraped and homogenized. Samples were centrifuged at 3,000×*g* for 5 min. The supernatant was extracted using the solid-phase extraction (SPE) method. The sample was loaded onto the Phenomenex Strata X (3 mL, 60 mg, 33 μm; Phenomenex, Torrance, California, USA) extraction cartridge, which was preconditioned by washing with 1 mL of acetonitrile and 1 mL of purified water. In the next step, the cartridge was washed out with 2 mL of 10 % (*v/v*) acetonitrile. Compounds of interest were eluted with 1 mL of acetonitrile. Samples were evaporated to dryness using vacuum concentrator. Dry samples were quantitatively reconstituted in the mixture of acetonitrile/water (30:70, *v/v*) by sonication. The solutions were mixed using a vortex for 5 min. One microliter of reconstituted samples was injected into the UHPLC/MS system.

UHPLC/MS/MS conditions

UHPLC/MS/MS chromatograms of samples were measured in the negative-ion ESI mode on a hybrid quadrupole-time-of-flight mass analyzer (micrOTOF-Q, Bruker Daltonics,

Germany). UHPLC was performed on an Agilent 1290 Infinity liquid chromatograph (Agilent Technology, Waldbronn, Germany) using Zorbax Eclipse C18 column 150×2.1 mm, 1.8 μm (Agilent Technology, Waldbronn, Germany), temperature 25 °C, flow rate 0.3 mL/min, and the injection volume 1 μL. The mobile phase consisted of 0.5 mM ammonium acetate adjusted to pH=4.0 (A) and acetonitrile (B). The linear gradient was as follows—0 min, 30 % B; 11 min, 95 % B; 12 min, 95 % B; and finally washing and reconditioning of the column. The quadrupole-time-of-flight (QqTOF) mass spectrometer with average resolving power higher than 13,000 was used with the following setting of tuning parameters—capillary voltage, 4.5 kV; drying temperature, 220 °C; the flow rate and pressure of nitrogen were 8 L/min and 1.3 bar, respectively. The external calibration was performed with sodium formate clusters before individual measurements. ESI mass spectra were recorded in the range of *m/z* 50–1,000 in the negative-ion mode. The isolation width Δ*m/z* 4 and the collision energy 20 eV (found as optimal energy for fragmentation of studied metabolite ions) using argon as the collision gas were used for MS/MS experiments.

Results and discussion

Detected in vitro metabolites were identified based on the presence of deprotonated molecules $[M\text{-}H]^-$ and the interpretation of their product ion spectra. The standards of potential metabolites were not synthesized due to their difficult synthesis. High mass accuracy measurement allows the confirmation of elemental composition and the type of metabolic reactions according to exact mass defects. Structures of possible metabolites were predicted using the MetabolitePredict software (Bruker Daltonics) and the knowledge of fragmentation behavior associated with metabolic reactions [9, 14, 15]. Various phase I metabolites can be expected in hepatocytes according to our previous in vitro studies [10, 11, 19, 20].

The total ion current chromatogram of sheep in vitro sample is shown in Fig. 2. Retention times, *m/z* values, molecular weights, elemental composition, and key fragment ions of MOP metabolites detected in MS/MS experiments are summarized in Table 1. All measurements discussed below were carried out in the negative-ion ESI mode, because this mode provides a better sensitivity for studied metabolites.

MS/MS spectrum of deprotonated molecule of parent drug (retention time, 8.5 min) at *m/z* 472 resulted in the abundant product ion at *m/z* 186. Similar results were reported by Kinsella et al. [7]. Key fragmentation patterns of all MOP metabolites formed during phases I and II biotransformation in sheep are summarized in Table 2 and Fig. 1. These product ions allow distinguishing of present substituents on the B ring. The proposed main metabolic pathways for MOP in ovine hepatocytes are shown in Fig. 4.

Phase I metabolites of MOP

Phase I biotransformation exposes or introduces a functional group and usually results in certain increase in the hydrophilicity of xenobiotics. Various oxidation, reduction, or hydrolysis reactions can be mentioned among possible phase I reactions of xenobiotics [21]. In case of MOP, products of S-oxidation, hydroxylation, and their combinations were identified as phase I metabolites in sheep (Fig. 4). All hydroxylation steps occur on the aromatic ring B. The position of oxidation and hydroxylation can be determined in different ways. The most reliable is the interpretation of MS/MS spectra of detected metabolites.

The S-oxidation and arene hydroxylation are two initial steps of MOP biotransformation. Sulfoxide of MOP (MOP.SO) was detected at *m/z* 488 $[M\text{-}H]^-$ in the negative-ion mode. This metabolite was converted to sulfone ($MOP.SO_2$; *m/z* 504 $[M\text{-}H]^-$ in the negative-ion mode) via further S-oxidation. $MOP.SO_2$ is the main MOP metabolite in sheep, and it represents the only MOP metabolite described previously by Kinsella [7]. Arene hydroxylation (MOP.OH) represented the second way of MOP phase I biotransformation. MOP.OH was detected at *m/z* 488 $[M\text{-}H]^-$ in the negative-ion mode. This metabolite was

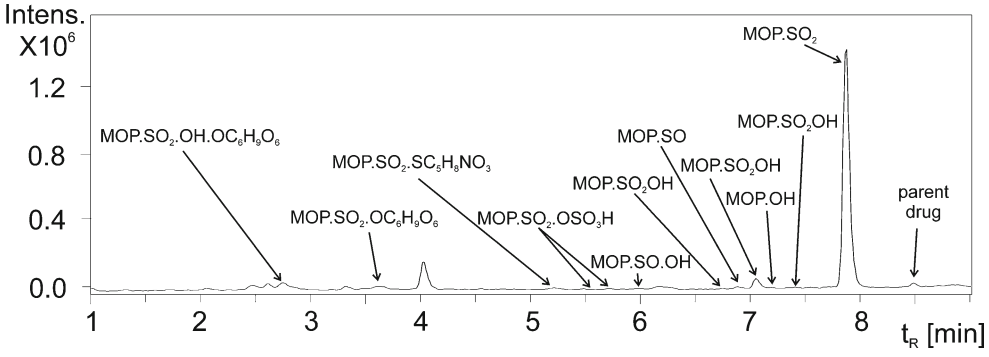

Fig. 2 Total ion current chromatogram of the sheep hepatocytes extract. *Arrows* show detected metabolites

Table 1 List of main peaks for monepantel biotransformation samples detected by UHPLC/MS/MS with their retention times, theoretical and experimental values of $[M\text{-}H]^-$ ions in ESI negative-ion mode, mass accuracies, molecular weights, elemental composition, product ions, and description of present metabolites

t_R [min] UHPLC	Important observed ions ESI-MS, *m/z*, $[M\text{-}H]^-$		Mass accuracy [ppm]	MW	Elemental composition	Description of metabolite formation		Product ions of $[M\text{-}H]^-$, *m/z*	Abbreviations
	Theoretical	Experimental				Phase I	Phase II		
2.6	712.0677	712.0668	−1.3	713	$C_{26}H_{21}F_6N_3O_{12}S$	2*S-oxidation, 2*hydroxylation	Glucuronidation	536; 394; 374; 354; 218	$MOP.SO_2OH.OC_6H_9O_6$
3.6	696.0728	696.0729	0.1	697	$C_{26}H_{21}F_6N_3O_{11}S$	2*S-oxidation, hydroxylation	Glucuronidation	520; 378; 358; 202	$MOP.SO_2.OC_6H_9O_6$
5.2	665.0605	665.0603	−0.3	666	$C_{25}H_{20}F_6N_4O_7S_2$	2*S-oxidation, hydroxylation	Conjugation with acetylcystein	638; 347; 186	$MOP.SO_2.SC_5H_8NO_3$
5.5	599.9975	599.9971	−0.7	601	$C_{20}H_{13}F_6N_3O_8S_2$	2*S-oxidation, hydroxylation	Sulfation	520; 202	$MOP.SO_2.OSO_3H$
5.7	599.9975	599.9979	0.7	601	$C_{20}H_{13}F_6N_3O_8S_2$	2*S-oxidation, hydroxylation	Sulfation	520; 202	$MOP.SO_2.OSO_3H$
6.0	504.0458	504.0462	0.8	505	$C_{20}H_{13}F_6N_3O_4S$	S-oxidation, hydroxylation	–	435; 202	MOP.SO.OH
6.7	520.0407	520.0399	−1.5	521	$C_{20}H_{13}F_6N_3O_5S$	2*S-oxidation, hydroxylation	–	493; 202	$MOP.SO_2.OH$
6.9	488.0509	488.0521	2.5	489	$C_{20}H_{13}F_6N_3O_3S$	S-oxidation	–	186; 166	MOP.SO
7.1	520.0407	520.0416	1.7	521	$C_{20}H_{13}F_6N_3O_5S$	2*S-oxidation, hydroxylation	–	493; 202; 182	$MOP.SO_2.OH$
7.2	488.0509	488.0505	−0.8	489	$C_{20}H_{13}F_6N_3O_3S$	Hydroxylation	–	202; 182	MOP.OH
7.4	520.0407	520.0417	1.9	521	$C_{20}H_{13}F_6N_3O_5S$	2*S-oxidation, hydroxylation	–	202; 182	$MOP.SO_2.OH$
7.9	504.0458	504.0455	−0.6	505	$C_{20}H_{13}F_6N_3O_4S$	2*S-oxidation	–	186; 166	$MOP.SO_2$
8.5	472.0560	472.0570	2.1	473	$C_{20}H_{13}F_6N_3O_2S$	–	–	186	MOP

consequently converted via S-oxidation to form the secondary metabolite (MOP.SO.OH; *m/z* 504 $[M\text{-}H]^-$ in the negative-ion mode). MS/MS spectra of two metabolites at *m/z* 488 (MOP.SO and MOP.OH) and *m/z* 504 ($MOP.SO_2$ and MOP.SO.OH) with the identical elemental composition are shown in Fig. 3. The different position of oxidation is easily recognized based on typical neutral losses. The presence of hydroxyl on the B ring is characterized by the fragment ion at *m/z* 202, whereas the oxidation on sulfur yields fragment ion at *m/z* 186 in accordance with the parent drug fragmentation.

MOP sulfone with arene hydroxylation ($MOP.SO_2.OH$) in various positions was identified in sheep. These metabolites, formed by two step S-oxidation and aromatic B hydroxylation, provided identical deprotonated molecules at *m/z* 520 $[M\text{-}H]^-$ in the negative-ion mode. In our experiments, three types of positional isomers were found. All positional isomers provide identical MS/MS spectra, and the position of hydroxylation cannot be distinguished based on mass spectra [22].

Another characteristic neutral losses for all phase I metabolites (except for MOP.SO.OH) were the hydrogen fluoride (Δ*m/z* 20) from the aromatic ring (B ring), for metabolites of MOP.SO and $MOP.SO_2$, ion *m/z* 166 $[186\text{-}HF]^-$, and for arene hydroxylation metabolites, ion *m/z* 182 $[202\text{-}HF]^-$, respectively. In case of MOP.SO.OH metabolite, the product ion at *m/z* 435 (Fig. 3) was formed via loss of trifluoromethyl group $[504\text{-}CF_3]^-$. The neutral loss of HCN (Δ*m/z* 27) was observed for $MOP.SO_2.OH$ metabolite in the fragment ion *m/z* 493 $[520\text{-}HCN]^-$. MOP metabolites with reduced carbonyl group were not found, although other anthelmintics with carbonyl group (flubendazole, mebendazole) undergo carbonyl reduction during biotransformation. In MOP, carbonyl group is probably stabilized by peptide bond and nitrile group.

All MOP phase I metabolites described above were found in 24-h incubations of MOP with the primary culture of ovine hepatocytes. Cytochrome P450 superfamily are the main enzymes that could catalyze MOP arene hydroxylation. These enzymes together with flavine monooxygenases could also be responsible for MOP S-oxidation [21], but the specific identification of participating enzymes will be matter of further study.

Phase II metabolites of MOP

Functional groups formed during phase I biotransformation are often sites of phase II biotransformation. Most phase II biotransformation reactions result in a significant increase in the hydrophilicity of metabolites, which greatly promotes the excretion of xenobiotics. In sheep in vitro samples, MOP glucuronides, sulfate, and acetylcysteine conjugates were found as products of MOP phase II biotransformation

Table 2 List of product ions and substituents of MOP metabolites of phase I and II biotransformation

Metabolite	Substituent R_1	Substituent R_2	Substituent R_3	Substituent R_4	Key fragment ions, *m/z*
MOP	–	–	H	H	186
MOP.SO	O	–	–	–	186
MOP.SO_2	O	O	–	–	186
MOP.OH	–	–	OH	–	202
MOP.SO.OH	O	–	OH	–	202
MOP.SO_2.OH	O	O	OH	–	202
MOP.SO_2.OH.$OC_6H_9O_6$	O	O	$OC_6H_9O_6$	OH	394
MOP.SO_2.$OC_6H_9O_6$	O	O	$OC_6H_9O_6$	–	378
MOP.SO_2.$SC_5H_8NO_3$	O	O	$SC_5H_8NO_3$	–	347

(Fig. 4). The glucuronidation is a major pathway of xenobiotic biotransformation in mammalian species except for the cat family. The glucuronidation requires the cofactor uridine diphosphate–glucuronic acid, and the reaction is catalyzed by UDP-glucuronosyltransferases. Glucuronide conjugates of xenobiotics and endogenous compounds are polar, water-soluble conjugates that are eliminated from the body in urine or bile. Many of xenobiotics and endogenous substrates that undergo *O*-glucuronidation also undergo sulfate conjugation. The sulfate conjugation generally produces a highly water-soluble sulfuric acid ester. This reaction is catalyzed by sulfotransferases, and the cofactor for the reaction is 3′-phosphoadenosine-5′-phosphosulfate. Many xenobiotic compounds are commonly conjugated with tripeptide glutathione through the action of glutathione S-transferases. Formed glutathione conjugates are unstable in many cases, and they are converted to conjugates with mercapturic acids (acetylcysteine) via the sequential cleavage of glutamic acid and glycine from the glutathione moiety, followed by *N*-acetylation of the resulting cysteine conjugate [21]. For the identification of MOP phase II conjugates, the similar fragmentation pattern as for phase I metabolites fragmentation were expected due to the similarity of molecular structures.

In ovine samples, the glucuronide of dihydroxylated MOP sulfone, MOP.SO_2.OH.$OC_6H_9O_6$, with deprotonated molecule at *m/z* 712 was found. Glucuronide of hydroxylated MOP sulfone, MOP.SO_2.$OC_6H_9O_6$, with *m/z* 696 [M-H]$^-$ was another detected MOP metabolite. The compound at *m/z* 665 [M-H]$^-$ was identified as MOP sulfone conjugated with acetylcysteine (MOP.SO_2.$SC_5H_8NO_3$). Two sulfates of hydroxylated MOP sulfone, MOP.SO_2.OSO_3H, at *m/z* 600 [M-H]$^-$ with different elution times were also detected in ovine hepatocytes.

Three metabolites (MOP.SO_2.OH.$OC_6H_9O_6$, MOP.SO_2.$OC_6H_9O_6$, MOP.SO_2.$SC_5H_8NO_3$) had similar product ions as the parent drug (*m/z* 186), but these metabolites differed by substituents on the aromatic B ring, which resulted in fragments *m/z* 394 for MOP.SO_2.OH.$OC_6H_9O_6$, *m/z* 378 for MOP.SO_2.$OC_6H_9O_6$, and *m/z* 347 for

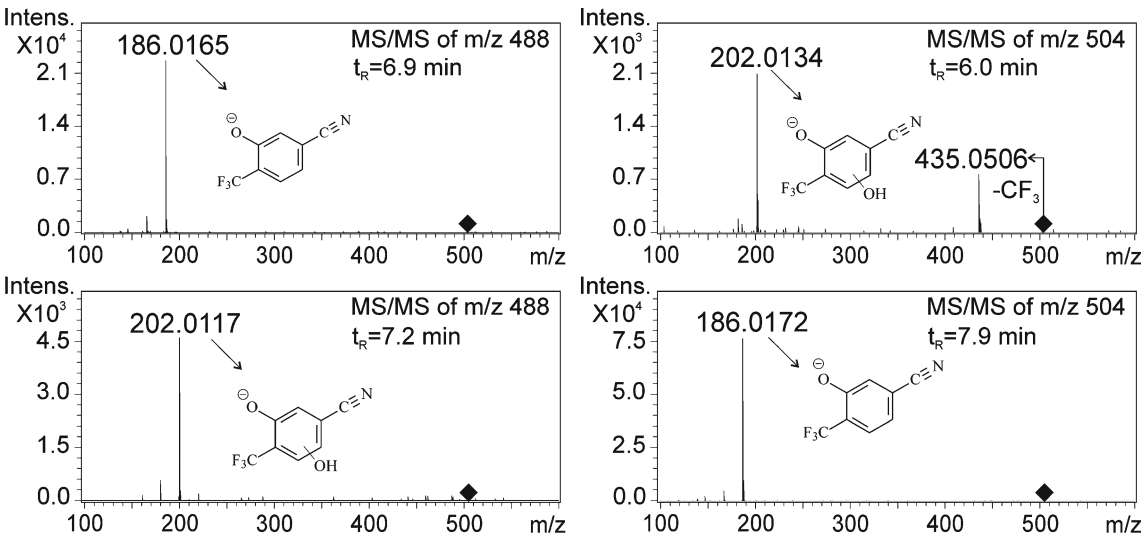

Fig. 3 Tandem mass spectra of [M-H]$^-$ ions *m/z* 488 and *m/z* 504 (see Table 1)

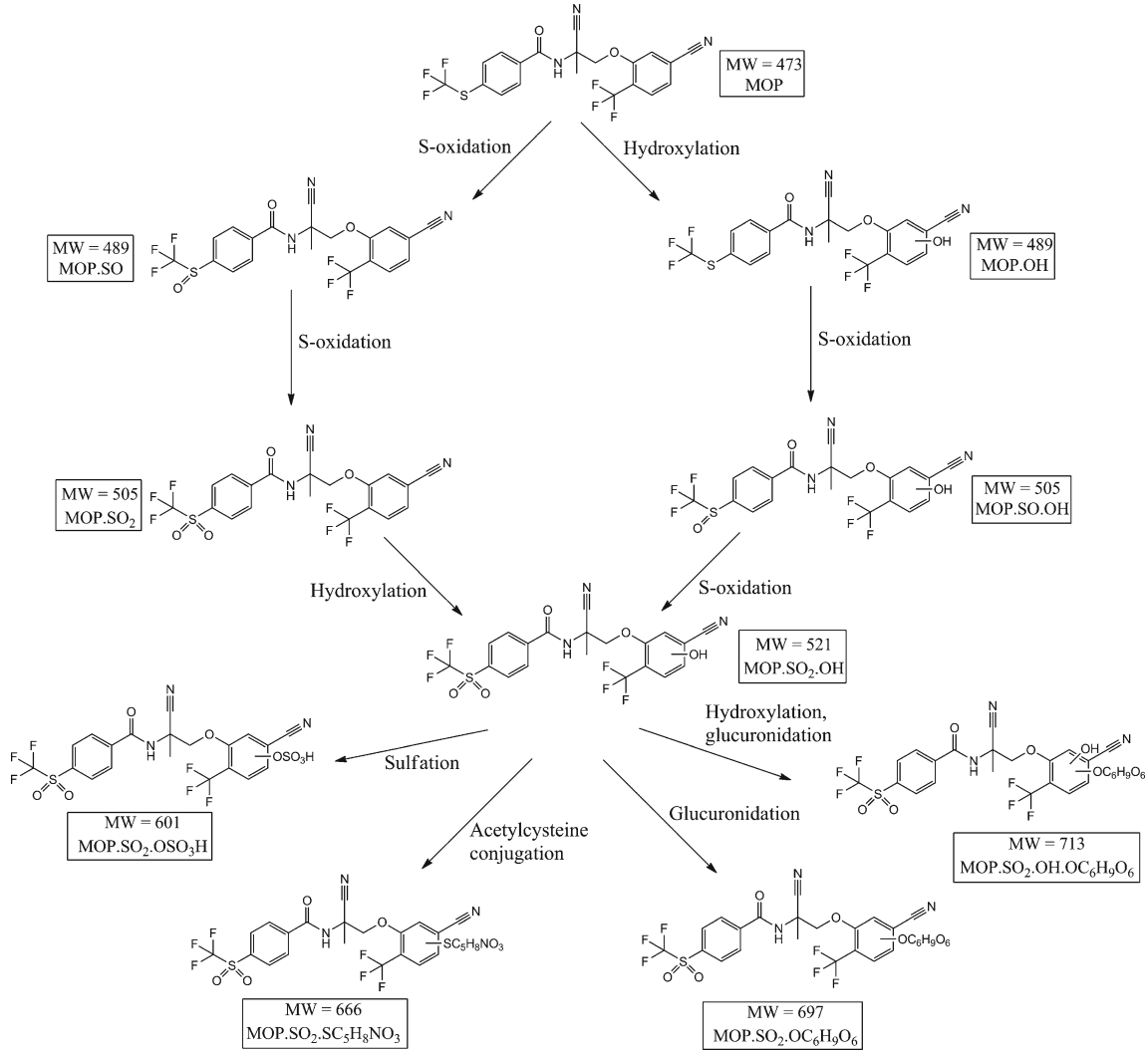

Fig. 4 Scheme of metabolic pathways of MOP in sheep in vitro study

$MOP.SO_2.SC_5H_8NO_3$ (Table 1). All metabolites of phase II biotransformation had similar product ion with characteristic losses of substituents on the aromatic B ring, at *m/z* 218 $[394\text{-}C_6H_8O_6]^-$ for $MOP.SO_2.OH.OC_6H_9O_6$, at *m/z* 202 $[378\text{-}C_6H_8O_6]^-$ for $MOP.SO_2.OC_6H_9O_6$, at *m/z* 186 $[347\text{-}SC_5H_8NO_3]^-$ for $MOP.SO_2.SC_5H_8NO_3$. Two metabolites ($MOP.SO_2.OH.OC_6H_9O_6$, $MOP.SO_2.OC_6H_9O_6$) had the same neutral loss of the anhydroglucuronic acid Δ*m/z* 176 from the aromatic B ring, at *m/z* 536 $[712\text{-}C_6H_8O_6]^-$ and at *m/z* 520 $[696\text{-}C_6H_8O_6]^-$, respectively. This is the characteristic neutral loss for all types of glucuronides [9, 23]. The identification of the conjugation site by MS is a difficult task, and the distinction is mostly achieved only for conjugation sites on different aromatic rings. Both metabolites had the characteristic neutral loss of hydrogen fluoride (Δ*m/z* 20) from the aromatic B ring, ion *m/z* 374 $[394\text{-}HF]^-$, and ion *m/z* 354 $[374\text{-}HF]^-$ for $MOP.SO_2.OH.OC_6H_9O_6$ and ion *m/z* 358 $[378\text{-}HF]^-$ for $MOP.SO_2.OC_6H_9O_6$, respectively. The product ion at *m/z* 520 $[600\text{-}SO_3]^-$ corresponds to sulfate of MOP sulfone ($MOP.SO_2.OSO_3H$). Only conjugate with acetylcysteine $MOP.SO_2.SC_5H_8NO_3$ had the neutral loss of HCN (Δ*m/z* 27) at *m/z* 638 $[665\text{-}HCN]^-$.

Conclusions

The aim of this study was to extend the knowledge of biotransformation of a new anthelmintic drug MOP in sheep. For this purpose, the incubation of MOP in the primary culture of ovine hepatocytes followed by SPE was used. All detected metabolites were identified using UHPLC/ESI-MS/MS technique in the negative-ion mode. The advantage of high mass accuracy measurements on QqTOF analyzer is the determination of elemental composition according to accurate *m/z* values of deprotonated molecules and their fragment ions. Typical neutral losses

allowed distinguishing the position of oxidation. Five MOP phase I metabolites and four phase II metabolites were detected in ovine hepatocytes. MOP biotransformation consisted of two-step S-oxidation, hydroxylation, sulfation, glucuronidation, and conjugation with glutathione followed by hydrolysis and acetylation resulting in MOP-conjugate with acetylcysteine. Obtained results demonstrate the ability of ovine hepatocytes to extensively metabolize MOP using both phase I and II phase biotransformation enzymes. Based on these results, the scheme of metabolic pathway of MOP in sheep has been proposed.

Acknowledgments This project was supported by the Czech Science Foundation (GA ČR, grant No. P502/10/0217), by the Grant Agency of Charles University (GA UK, grant No. 673612/B-CH/2012) and by the Charles University in Prague (research projects SVV 265 004).

References

1. Leathwick DM (2012) Modelling the benefits a new class of anthelmintic in combination. Vet Parasitol 186:93–100
2. Papadopoulos E (2008) Anthelmintic resistance in sheep nematodes. Small Rumin Res 76:99–103
3. Gobert NG, Jones MK (2008) Discovering new schistosome drug targets: the role of transcriptomics. Curr Drug Targets 9:922–930
4. Kaplan RM (2004) Drug resistance in nematodes of veterinary importance: a status report. Trends Parasitol 20:477–481
5. Kaminsky R, Ducray P, Jung M, Clover R, Rufener L, Bouvier J, Weber SS, Wenger A, Wieland-Berghausen S, Goebel T, Gauvry N, Pautrat F, Skripsky T, Froelich O, Komoin-Oka C, Westlund B, Sluder A, Mäser P (2008) A new class of anthelmintics effective against drug-resistant nematodes. Nature 452:176–180
6. Ducray P, Gauvry N, Pautrat F, Goebel T, Fruechtel J, Desaules Y, Weber SS, Bouvier J, Wagner T, Froelich O, Kaminsky R (2008) Discovery of amino-acetonitrile derivatives, a new class of synthetic anthelmintic compounds. Bioorg Med Chem Lett 18:2935–2938
7. Kinsella B, Byrne P, Cantwell H, McCormack M, Furey A, Danaher M (2011) Determination of the new anthelmintic monepantel and its sulfone metabolite in milk and muscle using a UHPLC-MS/MS and QuEChERS method. J Chromatogr B 879:3707–3713
8. Karadzovska D, Seewald W, Browning A, Smal M, Bouvier J, Giraudel JM (2008) Pharmacokinetics of monepantel and its sulfone metabolite, monepantel sulfone, after intravenous and oral administration in sheep. J Vet Pharmacol Ther 32:359–367
9. Holčapek M, Kolářová L, Nobilis M (2008) High-performance liquid chromatography-tandem mass spectrometry in the identification and determination of phase I and phase II drug metabolites. Anal Bioanal Chem 391:59–78
10. Vokřál I, Jedličková V, Jirásko R, Stuchlíková L, Bártíková H, Skálová L, Lamka J, Holčapek M, Szotáková B (2011) Metabolic fate of ivermectin in host (*Ovis aries*) and parasite (*Haemonchus contortus*). Vet Parasitol 185:168–174
11. Vokřál I, Jirásko R, Jedličková V, Bártíková H, Skálová L, Lamka J, Holčapek M, Szotáková B (2012) The inability of tapeworm *Hymenolepis diminuta* and fluke *Dicrocoelium dendriticum* to metabolize praziquantel. Vet Parasitol 185:168–174
12. Holčapek M, Jirásko R, Lísa M (2012) Recent developments in liquid chromatography-mass spectrometry and related techniques. J Chromatogr A 1259:3–15
13. Liu DQ, Hop CE (2005) Strategies for characterization of drug metabolites using liquid chromatography-tandem mass spectrometry in conjunction with chemical derivatization and on-line H/D exchange approaches. J Pharm Biomed Anal 37:1–18
14. Liu X, Jia L (2007) The conduct of drug metabolism studies considered good practice (I): analytical systems and in vivo studies. Curr Drug Metab 8:815–821
15. Jirásko R, Holčapek M, Nobilis M (2011) Identification of phase I and phase II metabolites of benfluron and dimefluron in rat urine using high-performance liquid chromatography/tandem mass spectrometry. Rapid Commun Mass Sp 25:2153–2162
16. Staack RF, Hopfgartner G (2007) New analytical strategies in studying drug metabolism. Anal Bioanal Chem 388:1365–1380
17. Berry MN, Edwards AM, Barritt GJ (1991) Laboratory techniques in biochemistry and molecular biology. In: Burdow RH, van Knippenberg PH (eds) Isolated hepatocytes preparation, properties and applications. Elsevier Science, Amsterdam, pp 15–35
18. Baliharová V, Velík J, Savlík M, Szotáková B, Lamka J, Tahotná L, Skálová L (2004) The effects of fenbendazole, flubendazole and mebendazole on activities of hepatic cytochromes P450 in pig. J Vet Pharmacol Ther 27:85–90
19. Velík J, Baliharová V, Skálová L, Szotáková B, Wsól V, Lamka J (2003) Stereospecific biotransformation of albendazole in muflon and rat-isolated hepatocytes. J Vet Pharmacol Ther 26:297–302
20. Montesissa C, Anfossi P, Van't Klooster G, Mengelers M (1996) The use of cultured hepatocytes from goats and cattle to investigate xenobiotic oxidative metabolism. Vet Res Commun 20:449–460
21. Parkinson A (2001) In: Klaassen CD (ed) Casarett & Doull's toxicology—the basic science of poisons. New York, McGraw-Hill
22. Nobilis M, Anzenbacher P, Pastera J, Svoboda Z, Hrubý K, Květina J, Ubik K, Trejtnar F (1996) Study of the biotransformation of a potential benzocfluorene antineoplastic using high-performance liquid chromatography with high-speed-scanning ultraviolet detection. J Chromatogr B 681:143–151
23. Holčapek M, Jirásko R, Lísa M (2010) Basic rules for the interpretation of atmospheric pressure ionization mass spectra of small molecules. J Chromatogr A 25:3908–3921